# *MIT Joint Program on the Science and Policy of Global Change*


## The Deep-Ocean Heat Uptake in Transient Climate Change

*Boyin Huang, Peter H. Stone, Andrei P. Sokolov and Igor V. Kamenkovich*

**Report No. 88**
***September 2002***

The MIT Joint Program on the Science and Policy of Global Change is an organization for research, independent policy analysis, and public education in global environmental change. It seeks to provide leadership in understanding scientific, economic, and ecological aspects of this difficult issue, and combining them into policy assessments that serve the needs of ongoing national and international discussions. To this end, the Program brings together an interdisciplinary group from two established research centers at MIT: the Center for Global Change Science (CGCS) and the Center for Energy and Environmental Policy Research (CEEPR). These two centers bridge many key areas of the needed intellectual work, and additional essential areas are covered by other MIT departments, by collaboration with the Ecosystems Center of the Marine Biology Laboratory (MBL) at Woods Hole, and by short- and long-term visitors to the Program. The Program involves sponsorship and active participation by industry, government, and non-profit organizations.

To inform processes of policy development and implementation, climate change research needs to focus on improving the prediction of those variables that are most relevant to economic, social, and environmental effects. In turn, the greenhouse gas and atmospheric aerosol assumptions underlying climate analysis need to be related to the economic, technological, and political forces that drive emissions, and to the results of international agreements and mitigation. Further, assessments of possible societal and ecosystem impacts, and analysis of mitigation strategies, need to be based on realistic evaluation of the uncertainties of climate science.

This report is one of a series intended to communicate research results and improve public understanding of climate issues, thereby contributing to informed debate about the climate issue, the uncertainties, and the economic and social implications of policy alternatives. Titles in the Report Series to date are listed on the inside back cover.

Henry D. Jacoby and Ronald G. Prinn,
*Program Co-Directors*


For more information, please contact the Joint Program Office

Postal Address: Joint Program on the Science and Policy of Global Change
77 Massachusetts Avenue
MIT E40-271
Cambridge MA 02139-4307 (USA)

Location: One Amherst Street, Cambridge
Building E40, Room 271
Massachusetts Institute of Technology

Access: Phone: (617) 253-7492
Fax: (617) 253-9845
E-mail: globalchange@mit.edu
Web site: http://MIT.EDU/globalchange/

# The Deep-Ocean Heat Uptake in Transient Climate Change

***Boyin Huang*, Peter H. Stone, Andrei P. Sokolov,***

***and Igor V. Kamenkovich*** [1]

Joint Program on the Science and Policy of Global Change
Massachusetts Institute of Technology

[1] Department of Atmospheric Sciences
University of Washington

(Submitted to *J. Climate*, May 2002)

* Corresponding author address:
Boyin Huang, 77 Massachusetts Avenue, Room 54-1721, Cambridge, MA 02139.
bhuang@wind.mit.edu.

## Abstract

The deep-ocean heat uptake (DOHU) in transient climate changes is studied using an ocean general circulation model (OGCM) and its adjoint. The model configuration consists of idealized Pacific and Atlantic basins. The model is forced with the anomalies of surface heat and freshwater fluxes from a global warming scenario with a coupled model using the same ocean configuration. In the scenario $CO_2$ concentration increases 1% per year. The heat uptake calculated from the coupled model and from the adjoint are virtually identical, showing that the heat uptake by the OGCM is a linear process.

After 70 years the ocean heat uptake is almost evenly distributed within the layers above 200 m, between 200 and 700 m, and below 700 m (about $20 \times 10^{22}$ J in each). The effect of anomalous surface fresh water flux on the DOHU is negligible. Analysis of CMIP-2 data for the same global warming scenario shows that qualitatively similar results apply to coupled atmosphere-ocean GCMs.

The penetration of surface heat flux to the deep ocean in our OGCM occurs mainly in the North Atlantic and the Southern Ocean, since both the sensitivity of DOHU to the surface heat flux and the magnitude of anomalous surface heat flux are large in these two regions. The DOHU relies on the reduction of convection and Gent-McWilliams mixing in the North Atlantic, and the reduction of Gent-McWilliams mixing in the Southern Ocean.

## 1. Introduction

The study of Levitus et al. (2000) shows that the world ocean has warmed since the mid-1950s. The change of deep-ocean temperature may be affected by the long-term climate variability. However, studies based on coupled atmosphere ocean general circulation models (AOGCMs) indicate that the detected warming is consistent with that expected due to an increase of greenhouse gases (Levitus et al. 2001; Barnett et al. 2001).

Studies from the Coupled Model Intercomparison Project (CMIP-2) show that the warming due to increasing greenhouse gases leads to an increase of downward net surface heat flux into the ocean. In addition, the warming is accompanied by an increase of freshwater flux into the ocean in higher latitudes, but out of the ocean in mid-latitudes (Fig. 1c-d). As a result, the thermohaline circulation slows down in most of the models. However, the relative role of the changes in surface heat and freshwater fluxes is unclear. Dixon et al. (1999) show that in the GFDL model the weakening of the thermohaline circulation is mainly caused by the increase of freshwater flux into the ocean. Their result seems to indicate the importance of freshwater flux to the thermocline circulation as in Weaver et al. (1993), Rahmstorf (1995 and 1996), Wiebe and Weaver (1999), and Zhang et al. (1999). On the other hand, the studies of Mikolajewicz and Voss (1999), and Kamenkovich et al. (2002a) indicate that the increase of net surface heat flux is the dominant factor in the slow-down of the thermohaline circulation.

From the viewpoint of deep-ocean heat uptake (DOHU, hereafter), the slow-down of the thermohaline circulation will cool the deep ocean due to reduced downward heat transport (Huang et al., 2002). What then causes the warming of the global deep ocean? As indicated in Huang et al. (2002), the DOHU in equilibrium may be sensitive to both the surface heat and freshwater fluxes. But, it is not clear whether they play an important role in the DOHU in transient climate changes. We will address this question by combining adjoint sensitivities to the surface heat and freshwater fluxes with anomalies of these fluxes from coupled AOGCM simulations when greenhouse gases increase. In an

earlier paper, we reported on the equilibrium sensitivities (Huang et al., 2002), but here we report on and make use of the transient sensitivities. Section 2 is a brief description of the MIT OGCM and its adjoint. The roles of anomalous surface heat and freshwater fluxes in DOHU in the MIT OGCM and the CMIP-2 models are compared in section 3. The sensitivity and mechanisms resulting in the increase of DOHU are studied in section 4. The spatial variations of DOHU due to the increase of greenhouse gases are presented in section 5. The DOHU below 200 and 700 m is briefly compared in section 6. Our conclusions are given in section 7.

## 2. Model

We use the MIT OGCM (Marshall et al. 1997) and its adjoint (Giering 1999) with an idealized Pacific and Atlantic connected by an idealized Drake Passage (Huang et al. 2002; Kamenkovich et al. 2002b). The longitudinal resolution is 1° near the western and eastern boundaries, but 4° in the central ocean. The finer resolution near the boundaries enables the simulation of western boundary current more realistically. The latitudinal resolution is 4°. The ocean depth is 4.5 km, which is discretized into 15 levels. The thickness between levels is 50 m near the surface, and increases to 550 m at the bottom. The diapycnal (vertical) diffusivity is set to $5\times10^{-5}\ m^2 s^{-1}$ for temperature and salinity. The isopycnal diffusivity is set to $10^3\ m^2 s^{-1}$, and the effect of mesoscale eddies on tracers is calculated based on Gent and McWilliams (1990) and Redi (1982). Isopycnal and thickness diffusivities are assumed to be the same.

The ocean is spun up for 5000 years by applying mixed boundary conditions:

$$\rho c_p \frac{dT_1}{dt}\Delta Z_1 = Q_S = \rho c_p \frac{SST - T_1}{\tau}\Delta Z_1 + F_H, \tag{1}$$

$$\frac{dS_1}{dt} = \frac{S_0}{\Delta Z_1} F_S, \tag{2}$$

$$F_S = E - P - R, \tag{3}$$

where SST is observed monthly sea surface temperature. $T_1$, $S_1$, and $\Delta Z_1$ are the temperature, salinity, and thickness of the first model layer. $\tau$ is a restoring time of 30 days. $F_H$ is observed monthly net surface heat flux (positive downward), and $F_S$ is observed annual freshwater flux, both from Jiang et al. (1999). $F_S$ is defined as the difference between evaporation, precipitation and river runoff. SST, $F_H$, and $F_S$ are zonally averaged in the Pacific and Atlantic separately. $S_0$ is the standard salinity of 35 psu.

After the spinup, the surface boundary condition of temperature is reset to the flux boundary condition as follows:

$$\rho c_p \frac{dT_1}{dt} \Delta Z_1 = \overline{Q}_S \tag{4}$$

where $\overline{Q}_S$ is monthly mean surface heat flux diagnosed from the last 10 years of the spinup run using (1). The flux boundary condition of (4) is very important in studying the adjoint sensitivity of DOHU to the surface heat flux. Otherwise, the perturbation added in (1) may immediately be damped by the restoring term except at the higher latitudes (Huang et al. 2002).

The adjoint of the MIT OGCM calculates the sensitivities of a so-called cost-function $F_c(n)$ at a time scale of *n* years to a set of model control parameters $P_m$:

$$S_m(n, x, y, z) = \frac{\partial F_c(n)}{\partial P_m(x, y, z)}, \ m = 1, M, \tag{5}$$

by applying the tangent linear and adjoint compiler (Giering 1999), which measures the change of the cost-function after a *constant* anomalous forcing maintained for *n* years at a specific location. The advantage of the adjoint is that the sensitivity to many parameters

($M >> 1$) can be calculated by one adjoint simulation. In our study, we choose the global averaged temperature below 700 m as a cost-function:

$$F_c = \overline{T}(n, z < -700m), \tag{6}$$

and choose surface heat flux ($Q_S$) and freshwater flux ($F_S$) as control parameters. The change of $F_c$ (in unit of °K) is referred to as DOHU unless otherwise specified. We ran the adjoint model for 70 years, and calculated the sensitivities of DOHU to $Q_S$ and $F_S$ for the time scales from 1 to 70 years as indicated in (5). Using these sensitivities, we will demonstrate that the impact of anomalous freshwater flux on the DOHU is negligible, and its effect on the thermohaline circulation is small as in Mikolajewicz and Voss (1999) and Kamenkovich et al. (2002a). We will not discuss the role of anomalous wind stress due to its small effect on the DOHU and the thermohaline circulation (Dixon et al. 1999; Mikolajewicz and Voss 1999; Bugnion 2001).

## 3. Role of surface heat and freshwater fluxes in the MIT model

### (a) Comparison using adjoint model

To estimate the role of surface heat and freshwater fluxes in the DOHU below 700 m in a global warming scenario, we use the anomalies of net surface heat flux ($Q_n$, $n = 1, \ 70$, positive downward) and freshwater flux ($F_n = \delta E_n - \delta P_n - \delta R_n$) when $CO_2$ concentration increases at 1% per year for 70 years. $Q_n$ and $F_n$ are averaged monthly from Kamenkovich et al. (2002b, KSS, hereafter). KSS use the modular ocean model of the Geophysical Fluid Dynamics Laboratory (GFDL) coupled with a zonal mean statistical-dynamical atmosphere. The ocean configuration of KSS is the same as in our study.

The DOHU at a time scale of *n* years forced by the anomaly of surface heat and freshwater fluxes can be estimated as

$$\Delta\overline{T}_n = \Delta T_n^Q + \Delta T_n^F = \sum_{i=1}^{n} \sum_{x,y} \left[ \frac{\partial \overline{T}_{n-i+1}}{\partial Q_S(x,y)} \Delta Q_i(x,y) + \frac{\partial \overline{T}_{n-i+1}}{\partial F_S(x,y)} \Delta F_i(x,y) \right] \quad (7)$$

Where

$$\Delta Q_n = Q_n - Q_{n-1}, \quad (8)$$

$$\Delta F_n = F_n - F_{n-1}, \quad n = 1, \ 70, \quad (9)$$

and $Q_n$ and $F_n$ are the anomalies of surface heat and freshwater fluxes from KSS (Fig. 1). The surface heat flux anomaly at year 70 is about 5 $Wm^{-2}$ in the Southern Ocean south of 45°S, and about 20 $Wm^{-2}$ in the North Atlantic north of 50°N (Fig.1a-b). The surface heat flux anomaly is very weak north of 30°S in the Pacific, and between 30°S and 30°N in the Atlantic. The precipitation dominates over evaporation by about 2 cm per year in the Southern Ocean south of 50°S, about 5 cm per year in the equatorial ocean between 10°S and 10°N in both the Pacific and the Atlantic, about 5 cm per year in the North Pacific north of 40°N, and about 10 cm per year in the North Atlantic north of 40°N (Fig. 1c-d). But the evaporation dominates over precipitation by about 5 cm per year between 40°S and 10°S and between 10°N and 40°N in both the Pacific and the Atlantic.

We find that the DOHU due to the anomalies of surface heat flux and freshwater flux at the time scale of 70 years is 0.052°K and –0.001°K, respectively (Table 1, KSS model). This indicates that the heat flux anomaly plays a dominant role over the freshwater flux anomaly in the DOHU below 700 m at this time scale in the global warming simulation of KSS. The effect of anomalous freshwater flux is negligible. We note that a one-degree change of average temperature below 700 m represents a DOHU of $3.7\times10^{24}$ J. The actual heat uptake calculated from the output of the KSS model simulation of the global warming scenario is 0.053°K (ΔT in Table 1). The closeness to

the value calculated using the adjoint sensitivities, 0.052 – 0.001 = 0.051, shows that the heat uptake in the KSS model is, to a very good approximation, a linear process.

**(b) Comparison using OGCM**

To further verify the predominance of surface heat flux anomaly in the DOHU in the global warming scenario, we designed a set of simulations with the MIT OGCM by introducing additional heat ( $Q_n$ ) and freshwater ( $F_n$ ) flux anomalies from KSS:

$$\rho c_p \frac{dT_1}{dt} \Delta Z_1 = Q_S = \overline{Q}_S + Q_n, \tag{10}$$

$$\frac{dS_1}{dt} = \frac{S_0}{\Delta Z_1}(F_S + F_n), \quad n = 1, \ 70, \tag{11}$$

where $\overline{Q}_S$ and $F_S$ are the climatological surface heat and freshwater fluxes as in (4) and (2). The simulations are run for 70 years in the following conditions: (A) control run without anomalies of surface heat and freshwater fluxes, $Q_n = F_n = 0$, (B) with heat flux anomaly only, $F_n = 0$, (C) with freshwater flux anomaly only, $Q_n = 0$, and (D) with both heat and freshwater flux anomalies, $Q_n \neq 0$ and $F_n \neq 0$.

The DOHU below 700 m is calculated by the difference between the perturbation and control simulations using

$$\Delta \overline{T}_n = \overline{T}_n^{pert}(z < -700m) - \overline{T}_n^{ctrl}(z < -700m). \tag{12}$$

The results show that the DOHU is about 0.05°K, -0.001°K, and 0.05°K (or 20, -1, and $19 \times 10^{22} J$ ), respectively, when forced with surface heat flux anomaly, freshwater flux anomaly, and the anomalies of both surface heat and freshwater fluxes from KSS. The dominant effect of anomalous surface heat flux on DOHU is consistent with the estimate using the adjoint sensitivities.

The anomalous heat flux increases the DOHU by the reduction of convection and Gent-McWilliams (1990) mixing (see section 4b for details), and decreases the thermohaline circulation. The anomalous freshwater flux in the high latitudes of the North Atlantic decreases the DOHU, albeit slightly, owing to the slow-down of the thermohaline circulation. The effect of excessive freshwater flux in the high latitudes is partially cancelled by the excessive evaporation in the subtropical Atlantic (Fig. 1d, KSS), as indicated in Latif et al. (2000). The reason is that the sensitivity of DOHU to the freshwater flux is positive over the entire Atlantic (not shown). Therefore, the excessive evaporation in these latitudes can increase the DOHU below 700 m. It can also intensify the strength of thermohaline circulation due to its positive sensitivity to the freshwater flux over the entire Atlantic as indicated in Bugnion (2001).

The OGCM calculations show that the thermohaline circulation in the North Atlantic is reduced by about 5, 1, and 6 Sv ($1Sv = 10^6 m^3 s^{-1}$), respectively, when forced with surface heat flux anomaly only, freshwater flux anomaly only, and the anomalies of both surface heat and freshwater fluxes. Indeed, the effect of anomalous surface heat flux on the thermohaline circulation dominates over that of the freshwater flux as demonstrated by Kamenkovich et al. (2002). This is consistent with the result in Mikolajewicz and Voss (2000) using the ECHAM3 model, but different from Dixon et al. (1999) using the GFDL model.

**(c) Comparison of buoyancy forcing**

Figure 1 shows the changes in the surface heat and moisture fluxes after 70 years of the global warming scenario with the KSS model. This figure also includes results from seven CMIP-2 models, those from the Bureau of Meteorology Research Centre in Australia (MBRC1, Power et al. 1993), the Max Planck Institute in Hamburg, Germany (ECHAM3, Cubasch et al. 1997; Voss et al. 1998), the Geophysical Fluid Dynamics Laboratory (GFDL, Manabe et al. 1991; Manabe and Stouffer 1996), the Goddard

Institute for Space Studies (GISS, Russell et al. 1995; Russell and Rind 1999), the Institute of Atmospheric Physics in China (IAP, Wu et al. 1997; Zhang et al. 2000), the National Center for Atmospheric Research (NCAR-CSM, Boville and Gent 1998), and the United Kingdom Meteorological Office (HadCM2, Johns 1996; Johns et al. 1997). We note that the positions of maximum and minimum E-P-R in the North Atlantic in KSS are slightly different from those in the CMIP-2 models.

However the dominance of the surface heat flux anomaly over the freshwater flux anomaly in the MIT models seems to be consistent with the buoyancy flux anomalies in the CMIP-2 models. As shown in Figure 2, the buoyancy forcing due to the anomalous surface heat flux decreases about $6\times10^{-7}\,Kgm^{-2}s^{-1}$ in the North Atlantic north of 50°N except for the NCAR-CSM model (Fig. 2b). But, the buoyancy forcing due to excessive precipitation decreases merely about $0.5\times10^{-7}\,Kgm^{-2}s^{-1}$ in the North Atlantic north of 50°N (Fig. 2d). For example, the buoyancy forcing due to the surface heat and freshwater fluxes between year 60 and 80 between 45°N and 73°N is about –1.75 and –$0.74\times10^{-9}\,Kgm^{-2}s^{-1}$, respectively, in the ECHAM3 model (refer to Fig. 11 of Mikolajewicz and Voss 2000).

As a test of whether the DOHU sensitivities of the MIT adjoint model are reasonably consistent with those of the CMIP-2 models, we use them to estimate DOHU in the CMIP-2 models, and compare the estimates with DOHU calculated directly from the CMIP-2 data. To make the estimates we average the CMIP-2 surface flux anomalies zonally, but separately for the Pacific and Atlantic basins, and combine them with the adjoint model sensitivities. The results are shown in Table 1. They suggest that, as in our models, DOHU due to anomalous freshwater is very small in the CMIP-2 models.

Table 1 also shows DOHU calculated directly from the CMIP-2 data (ΔT in the table). The model differences are notable (they range from 0.03K to 0.09K), and represent one reason for the differences between simulations of climate change with different state-of-the-art coupled GCMs (Sokolov and Stone, 1998). Figure 3 illustrates

the correlation between DOHU estimated using the MIT adjoint model sensitivities and the actual simulated DOHU. The correlation coefficient, excluding the KSS model, is 0.69, which is significant at the 95% confidence level. Thus the sensitivities of the MIT adjoint model, in spite of its simplifications compared to the CMIP-2 models, appear to be qualitatively similar to those of state-of-the-art coupled GCMs.

## 4. Sensitivity and mechanisms of deep-ocean heat uptake

### (a). Sensitivity

As indicated in (5), the sensitivity of DOHU to the net surface heat ($Q_S$) and freshwater ($F_S$) fluxes obviously depends on the time scale upon which the anomalous forcing acts. In our study of the DOHU below 700 m at the time scale of 70 years, we run the adjoint model for 70 years, and calculate the sensitivities for the time scale from 1 to 70 years. Figure 4 displays the sensitivity of DOHU to the surface heat flux at the time scale of 50 years. The sensitivity of DOHU to the surface heat flux is positive in both the Pacific and Atlantic except in a small area of the southwestern South Atlantic near the Drake Passage. The positive sensitivity indicates that the heat absorbed at the surface will in part penetrate into the deep ocean and increase the global mean temperature below 700 m. However, the magnitude of the sensitivity is generally larger in the North Atlantic (about $5-20\times10^{-6}\,Km^2W^{-1}$) than in the North Pacific (about $5\times10^{-6}\,Km^2W^{-1}$), but smaller in the South Atlantic (less than $5\times10^{-6}\,Km^2W^{-1}$) than in the South Pacific between 0° and 50°S (about $5-10\times10^{-6}\,Km^2W^{-1}$). The sensitivity in the Southern Ocean is the highest (about $20-30\times10^{-6}\,Km^2W^{-1}$).

### (b). Mechanisms

As shown in section 3, the DOHU below 700 m in the global warming scenario of a 1% $CO_2$ increase per year is mainly determined by the anomaly of surface heat flux. A further question is: How does the surface heat flux penetrate into the deep ocean?

Obviously, the increase of the DOHU below 700 m must be associated with the increase of the net heat flux ($Q_{net}$) across 700 m. The net heat flux is the sum of the advective heat flux ($Q_W$), convective heat flux ($Q_{CV}$), diapycnal (vertical) diffusive heat flux ($Q_{DD}$), and diffusive heat flux (isopycnal and thickness diffusion) due to Gent-McWilliams (1990) mixing ($Q_{GM}$), as in Huang et al. (2002). These heat fluxes are all defined as positive downward, and formulated as follows:

$$Q_W = \rho c_p \iint WT dxdy , \tag{13}$$

$$Q_{CV} = \frac{\rho c_p \Delta z_i}{\Delta t}(T_i - \frac{T_i \Delta z_i + T_{i+1}\Delta z_{i+1}}{\Delta z_i + \Delta z_{i+1}}) , \tag{14}$$

$$Q_{DD} = \rho c_p \iint K_t \frac{\partial T}{\partial z} dxdy , \tag{15}$$

$$Q_{GM} = 2\rho c_p \iint I_t \left[ \frac{\partial T}{\partial y}\left(\frac{\partial z}{\partial y}\right)_\sigma + \frac{\partial T}{\partial x}\left(\frac{\partial z}{\partial x}\right)_\sigma \right] dxdy , \tag{16}$$

$$Q_{net} = Q_W + Q_{CV} + Q_{DD} + Q_{GM} . \tag{17}$$

Here $K_t$ and $I_t$ are diapycnal (vertical) and isopycnal diffusitivities of temperature. $(\partial z / \partial y)_\sigma$ is the slope of the isopycnal surface. The convective heat flux is calculated according to the adjustment of ocean temperature within the adjacent layers when water density is higher in the upper layer than in the lower layer.

To diagnose what physical processes are involved in the DOHU, we take advantage of the adjoint model using these five heat fluxes as the cost-functions, and calculate the adjoint sensitivities of these five heat fluxes to the surface heat flux ($Q_S$) as indicated in (5). Figure 5 shows these sensitivities for the time scale of 50 years. It is clear that the sensitivity of $Q_{net}$ across 700 m to $Q_S$ is positive (Fig. 5a), and is strong in the North Atlantic (about $120 \times 10^9 m^2$) and the Southern Ocean (about $60-80 \times 10^9 m^2$).

The sign and magnitude of the sensitivity of $Q_{net}$ to $Q_S$ in Figure 5a are very consistent with those of the sensitivity of DOHU to $Q_S$ in Figure 4. When the ocean surface is forced with a heat flux anomaly, the downward net heat flux across 700 m will increase, and therefore the deep ocean takes up more heat.

Furthermore, the increase of $Q_{net}$ across 700 m is mainly associated with convective heat flux ($Q_{CV}$) in the North Atlantic and the eddy heat flux ($Q_{GM}$) due to Gent-McWilliams mixing in the Southern Ocean and the North Atlantic. This can be seen by comparing the sign and magnitude of their sensitivities in Figures 5a, 5c, and 5e. When the surface heat flux increases, the upper layer ocean becomes lighter, and therefore convection is prohibited. This means that upward convective heat flux decreases or downward anomaly of convective heat flux increases in the North Atlantic. Since $Q_{GM}$ is directly associated with the slope of the isopycnal surface as indicated in (16), upward $Q_{GM}$ mainly occurs in the North Atlantic and the Southern Ocean (not shown) where the slope of the isopycnal surface is very steep. When the surface heat flux increases in these regions, the slope of the isopycnal surface will be flattened. Therefore, upward eddy heat flux due to Gent-McWilliams mixing decreases or downward anomaly of eddy heat flux increases.

The positive sensitivities of net, advective, diapycnal diffusive heat fluxes to the surface heat anomaly in the South Pacific (Figs. 5a, 5b, and 5d) indicate that the vertical advection ($Q_W$) and diapycnal diffusion may also contribute to the net heat flux across 700 m. Nevertheless, their effects on the DOHU appear to be small, since the magnitude of anomalous surface heat flux is very small in the South Pacific (Fig. 6b). Overall, the global mean sensitivities of $Q_{net}$, $Q_W$, $Q_{CV}$, $Q_{DD}$, and $Q_{GM}$ to the surface heat flux are about 40, 2, 7, 3, and $27\times10^9 m^2$, respectively, at the time scale of 50 years, indicating that the DOHU is mainly associated with the reduction of upward Gent-McWilliams mixing.

In addition, we can see that the distribution of $Q_W$ sensitivity to the surface heat flux $Q_S$ (Fig. 5b) is directly associated with the change of the thermohaline circulation (Bugnion 2001; Mikolajewicz and Voss 2000; Dixon et al. 1999). As the surface heat flux increases in the Atlantic, we speculate that the conveyor circulation of downwelling in the Atlantic and upwelling in the Pacific decreases. Therefore, downward advective heat flux will decrease in the Atlantic, which will lead to a cooling of the deep ocean. In contrast, when the surface heat flux increases in the Pacific, the conveyor circulation will increase. Therefore, downward advective heat flux will increase, which will result in a warming of the deep ocean.

Since the effect of anomalous freshwater flux on DOHU is negligible in this global warming scenario, we do not discuss the detailed mechanisms by which the freshwater flux affects DOHU. Readers may refer to a similar discussion in Huang et al. (2002) about the mechanisms of DOHU due to freshwater flux for equilibrium states.

## 5. Characteristics of deep-ocean heat uptake

Calculations in section 3a-b indicate that in our global warming simulations after 70 years the total heat absorbed by the ocean is about $60\times10^{22}J$, and the DOHU below 700 m is about $20\times10^{22}J$. A further question is, how is the DOHU distributed within the horizontal ocean domain? We answer this question by using our adjoint sensitivities with the actual surface heat flux changes calculated with the KSS model:

$$E(x,y)=\frac{\rho c_p V_{700}}{\Delta x\Delta y}\sum_{i=1}^{n}\left[\frac{\partial\overline{T}_{n-i+1}}{\partial Q_S(x,y)}\Delta Q_i+\frac{\partial\overline{T}_{n-i+1}}{\partial F_S(x,y)}\Delta F_i\right],\ n=1,\ \ 70. \tag{18}$$

Here, $E(x,y)$ is the DOHU per unit area. $V_{700}$ is the ocean volume below 700 m, and $\Delta Q_i$ and $\Delta F_i$ are from (8) and (9). The effect from the wind stress anomaly is neglected. Figure 6a displays the spatial distribution of the accumulated heat penetrated across 700

m within 70 years. We can see that the penetration of heat mainly occurs in the North Atlantic north of 40°N (about $2-15\times10^{9}\,Jm^{-2}$), the South Atlantic south of 50°S (about $2-6\times10^{9}\,Jm^{-2}$), and the South Pacific south of 45°S (about $2-4\times10^{9}\,Jm^{-2}$). It appears that the surface heat flux has difficulty penetrating across 700 m into the deep ocean in a large area of the Pacific north of 40°S and the central Atlantic between 50°S and 30°N. Indeed, the total heat uptake from the atmosphere within 70 years (Fig. 6b) in the Pacific north of 40S (about $2-4\times10^{9}\,Jm^{-2}$) and the central Atlantic (about $1-2\times10^{9}\,Jm^{-2}$) is also very weak if compared with that over the North Atlantic (about $10-45\times10^{9}\,Jm^{-2}$) and the Southern Ocean (about $4-8\times10^{9}\,Jm^{-2}$). Therefore, we can think of a heat sink in the North Atlantic and the South Ocean.

We speculate that the heat sink in our OGCM with an idealized basin may be similar in fully coupled GCMs, although its strength and width distribution will not be identical. For example, as indicated in Figure 1a-b, the heat flux anomaly at the ocean surface is mainly located in the North Atlantic north of 50°N and the Southern Ocean south of 40°S in almost all fully coupled GCMs with realistic topography, as well as in the coupled model with an idealized basin from KSS. However, a weak heat sink may also exist in the North Pacific north of 50°N such as in the study of Gregory (2000) using the HadCM2 model as indicated in Figure 1a.

Next we compare the heat uptake below 700 m with total absorbed heat,

$$R_n = \frac{DOHU}{Q_0},\ \ n = 1,\ \ 70, \tag{19}$$

where

$$Q_0 = \int \sum_{i=1}^{n} Q_i \Delta t_i \, dxdy, \tag{20}$$

is the total heat absorbed by the ocean within $n$ years, $Q_i$ is the heat flux anomaly at year $i$, and $\Delta t_i$ is the time interval between the model outputs of $Q_i$ and $Q_{i+1}$. In the adjoint model, DOHU is estimated as

$$DOHU = \int E(x, y)dxdy \,, \tag{21}$$

which is the global integration of (18). Calculation indicates that the ratio $R_n$ is about 10-20% during years 10-20, and gradually increases to about 33% as indicated in Figure 7a. The large fluctuation of the ratio in the first 10 years is purely due to the fact that $Q_0$ is almost near zero, and the ratio is very noisy.

The ratio estimated from the adjoint model is confirmed by the simulation of the MIT OGCM and the original simulation of KSS, where the DOHU is calculated using

$$DOHU = \rho c_p V_{700} \Delta \overline{T}_n \,. \tag{22}$$

Here, $\Delta \overline{T}_n$ is the mean temperature difference below 700 m between the perturbation and control run as shown in (12). It is clear that the ratio $R_n$ is very close in all three models. The ratios $R_n$ in the original simulation of the fully coupled GCMs from CMIP-2 with a realistic topography are also calculated using equations (12), (19) and (22), since the heat uptake due to the change of sea-ice heat content is trivial and neglected. These ratios are about 10-30% during the first 20 years, and gradually increase to about 20-40% during the fourth 20 years (Fig. 7b). The fluctuation of these ratios might be associated with different vertical diffusivities applied in these models.

## 6. Heat uptake below 200 m

The characteristics of the DOHU below 200 m in the global warming scenario with a 1% $CO_2$ increase per year for 70 years are very similar to those of the DOHU below 700 m. The DOHU below 200 m (about 0.1°K) based on the adjoint sensitivities

and OGCM simulation with an idealized basin are again very close (Table 1), indicating the linearity of the response of DOHU to the surface heat flux. The DOHU estimated in the idealized basin is in the middle of that calculated in the realistic basin of the CMIP-2 models (about 0.06-0.15°K). The DOHU estimated by applying the adjoint sensitivity is again well correlated with that calculated in the coupled models of CMIP-2 (Fig. 8). The correlation excluding the KSS model is 0.73, which corresponds to a better than 95% confidence level. Again the effect of anomalous surface freshwater flux on the DOHU below 200 m appears to be negligible (Table 1).

The adjoint sensitivity of DOHU below 200 m to the surface heat flux is positive over both the Pacific and the Atlantic (Fig. 9) as for the sensitivity of the DOHU below 700 m in Figure 4. The main difference is that the magnitude of sensitivity of the DOHU below 200 m is higher and more uniformly distributed than that of the DOHU below 700 m.

The mechanisms by which the surface heat flux penetrates across 200 m (not shown) are similar to those across 700 m. The heat flux across 200 m is associated in part with the reduction of convection in the North Atlantic, which is consistent with Gregory (2000). However, Gregory (2000) shows that the increase of vertical diffusion contributes a lot to the heat flux near 200 m in both the North Pacific and North Atlantic, which differs from our result. Rather our study indicates that the reduction of the Gent-McWilliams mixing is the main contributor to the vertical heat flux in the North Atlantic. This may be associated with the different subgridscale eddy parameterizations: i.e., Gregory (2000) used a diapycnal diffusion with its coefficient increasing with depth, and we use Gent-McWilliams mixing in addition to diapycnal diffusion with a constant coefficient.

The spatial distribution of DOHU below 200 m can be plotted based on its adjoint sensitivity as indicated in (18) and is shown in Figure 10. It mainly occurs in the regions of the heat sink in the North Atlantic and in the Southern Ocean just as for the DOHU

below 700 m. However, the magnitude of DOHU increases to $30 \times 10^9 \, Jm^{-2}$ in the North Atlantic north of 40°N and to $4-6 \times 10^9 \, Jm^{-2}$ in the Southern Ocean south of 40°S.

The ratio of heat uptake below 200 m to the total heat uptake is shown in Figure 11. The ratios of DOHU estimated in the adjoint model, MIT OGCM, and KSS model are very close; they are about 20-50% at the time scale of 10 years and gradually increase to about 70% at the time scale of 70 years (Fig. 11a). These ratios are also consistent with those from the fully coupled GCMs of CMIP-2 (Fig. 12b), which range from 10 to 60% at 10-year time-scale and from 60 to 70% at 70-year time-scale. The surface heat flux into the ocean in this global warming scenario is almost equally (about one-third) absorbed by the upper ocean above 200 m, between 200 and 700 m, and below 700 m. These ratios are close to those in the study of Gregory (2000).

## 7. Conclusions

We have studied the DOHU using simulations with the MIT OGCM and its adjoint with an idealized geometry. The simulations are forced with the anomalous surface heat and freshwater fluxes from the coupled model of KSS in a global warming scenario where atmospheric $CO_2$ increases 1% per year for 70 years. The DOHU in our simulations are compared with that in the fully coupled AOGCMs of CMIP-2.

We find that the contribution of anomalous freshwater fluxes to DOHU in our models is negligible. This is in part due to the relatively small contribution of the freshwater flux anomalies to the buoyancy flux anomalies in the KSS global warming scenario. We found that the buoyancy flux anomalies in all the CMIP-2 coupled GCMs were also dominated by the heat flux anomalies, and that the DOHU in the CMIP-2 models were well correlated with DOHU estimates based on the MIT adjoint model sensitivities. Thus the DOHU in the CMIP-2 models appears to have qualitatively similar sensitivities.

The sensitivity of DOHU to the downward surface heat flux in the ajoint model is positive in both the Pacific and Atlantic, but it is strongest in the North Atlantic and the Southern Ocean. The increase of DOHU is largely associated with the reduction of convective activity due to surface heating and the reduction of Gent-McWilliams mixing due to flattening of the isopycnal slopes in the North Atlantic. The reduction of Gent-McWilliams mixing is the main contributor to the increase of the DOHU in the Southern Ocean. The dominance of the heat sinks in these two regions arises because the sensitiviy of DOHU to heat flux perturbations in these areas and the anomalies in the surface heat fluxes in the global warming scenario are both particularly large in these regions. We would expect qualitatively similar heat sinks to occur in coupled GCMs with similar physics.

The heat absorption of the ocean in our models is almost equally (one-third) distributed above 200 m, between 200 and 700 m, and below 700 m. After 70 years of the global warming scenario the DOHU below 700 m is about $20 \times 10^{22}$ J, or 0.05 K. In the coupled GCMs of CMIP-2, this latter number varies from 0.03 to 0.09 K. In the MIT OGCM the heat uptake in the 70 years of the global warming scenario is to a very good approximation a linear response to the surface heat flux changes.

**References**


Barnett, T. P., D. W. Pierce, and R. Schnur, 2001: Detection of anthropogenic climate change in the world's oceans, *Science*, **292**, 270-274.

Boville, B. A., and P. R. Gent, 1998: The NCAR Climate System Model, Version One. *J. Climate,* **11**, 1115-1130.

Bugnion, V., *Driving the ocean's overturning: Analysis with adjoint models*, Ph.D. dissertation, Massachusetts Institute of Technology, 179 pp., 2001, available at Lindgren Library, MIT Building 54, 77 Massachusetts Ave., Cambridge, MA-02139.

Cubasch, U., R. Voss, G. C. Hegerl, J. Waszkewitz, and T. J. Crowley, 1997: Simulation of the influence of solar radiation variations on the global climate with an ocean-atmosphere general circulation model. *Climate Dyn*., **13**, 757-767.

Dixon, K. W., T. L. Delworth, M. J. Spelman, and R. J. Stouffer, 1999: The influence of transient surface fluxes on North Atlantic overturning in a coupled GCM climate change experiment, *Geophys. Res. Lett*., **26**, 2749-2752.

Gent, P. R., and J. C. McWilliams, 1990: Isopycnal mixing in ocean circulation model, *J. Phys. Oceanogr*., **20**, 150-155.

Giering, R., 1999: *Tangent linear and adjoint model compiler*, *Users manual*, Max-Planck Institut, Hanburg, Germany, 64 pp.

Gregory, J. M., 2000: Vertical heat transports in the ocean and their effect on time-dependent climate change, *Climate Dyn*., **16**, 501-515.

Huang, B., P. H. Stone, and C. Hill, 2002: Sensitivities of deep-ocean heat uptake and heat content to the surface fluxes and subgrid-scale parameters in an OGCM with idealized geometry, *J. Geophys. Res*., in press.

Jiang, S., P. H. Stone, and P. Malanotte-Rizzoli, 1999: An assessment of the Geophysical Fluid Dynamics Laboratory ocean model with coarse resolution: Annual-mean climatology, *J. Geophys. Res.*, **104**, 25,623-25,645.

Johns. T. C., 1996: A description of the Second Hadley Centre Coupled Model (HadCM2). *Climate Research Technical Note 71*, Hadley Centre, United Kingdom Meteorological Office, Bracknell Berkshire RG12 2SY, United Kingdom, 19 pp.

Johns, T. C., R. E. Carnell, J. F. Crossley, J. M. Gregory, J. F. B. Mitchell, C. A. Senior, S. F. B. Tett, and R. A. Wood, 1997: The second Hadley Centre coupled ocean-atmosphere GCM: Model description, spinup and validation. *Climate Dyn.*, **13**, 103-134.

Kamenkovich, I. V., A. Sokolov, and P. H. Stone, 2002a: Feedbacks affecting the response of the thermohaline circulation to increasing CO2: A study with a model of intermediate complexity, submitted to *Clim. Dyn*.

Kamenkovich, I. V., A. Sokolov, and P. H. Stone, 2002b: A coupled atmospheric-ocean model of intermediate complexity for climate change, *Clim. Dyn.*, in press.

Latif, M., E. Roeckner, U. Mikolajewicz, and R. Voss, 2000: Tropical stabilization of the thermohaline circulation in a greenhouse warming simulation, *J. Climate*, **13**, 1809-1813.

Levitus, S., J. I. Antonov, T. P. Boyer, and C. Stephens, 2000: Warming of the world ocean, *Science*, **287**, 2225-2229.

Levitus, S., J. I. Antonov, J. Wang, T. L. Delworth, K. W. Dixon, and A. J. Broccoli, 2001: Anthropogenic warming of earth's climate system, *Science*, **292**, 267-270.

Manabe, S., R. J. Stouffer, M. J. Spelman, and K. Bryan, 1991: Transient responses of a coupled ocean-atmosphere model to gradual changes of atmospheric CO2. Part I: Annual mean response. *J. Climate*, **4**, 785-818.

Manabe, S., and R. J. Stouffer, 1996: Low-frequency variability of surface air temperature in a 1000-year integration of a coupled atmosphere-ocean-land surface model. *J. Climate*, **9**, 376-393.

Marshall, J., A. Adcroft, C. Hill, L. Perelman, and C. Heisey, 1997: A finite volume, incompressible Navier Stokes model for studies of the ocean on parallel computers, *J. Geophys. Res.*, **102**, 5753-5766.

Mikolajewicz, U., and R. Voss, 2000: The role of the individual air-sea flux components in CO2-induced changes of the ocean's circulation and climate, *Clim. Dyn*., **16,** 627-642.

Power, S. B., R. A. Colman, B. J. McAvaney, R. R. Dahni, A. M. Moore, and N. R. Smith, 1993: The BMRC Coupled atmosphere/ocean/sea-ice model. *BMRC Research Report No. 37*, Bureau of Meteorology Research Centre, Melbourne, Australia, 58 pp.

Rahmstorf, S., 1995: Bifurcation of the Atlantic thermohaline circulation in response to changes in the hydrological cycle, *Nature,* **378**, 145-149.

Rahmstorf, S., 1996: On the freshwater forcing and transport of the Atlantic thermohaline circulation, *Clim. Dyn.,* **12**, 799-811.

Rahmstorf, S., and A. Ganopolski, 1999: Long-term global warming scenarios computed with an efficient coupled climate model, *Climatic Change*, **43**, 353-367.

Redi, M. H., 1982: Oceanic isopycnal mixing by coordinate rotation, *J. Phys. Oceanogr.*, *12*, 1154-1158.

Russell, G. L., J. R. Miller, and D. Rind, 1995: A coupled atmosphere-ocean model for transient climate change studies. *Atmos.-Ocean*, **33**, 683-730.

Russell, G. L., and D. Rind, 1999: Response to $CO_2$ transient increase in the GISS coupled model: Regional coolings in a warming climate. *J. Climate*, **12**, 531-539.

Sokolov, A., and P. H. Stone, 1998: A flexible climate model for use in integrated assessments. *Climate Dynamics,* **14,** 291-303.

Voss, R., R. Sausen, and U. Cubasch, 1998: Periodically synchronously coupled integrations with the atmosphere-ocean general circulation model ECHAM3/LSG. *Climate Dyn.,* **14**, 249-266.

Weaver, A., J. Marotzke, P. E. Cummins, and E. S. Sarachik, 1993: Stability and variability of the thermohaline circulation, *J. Phys. Oceanogr.,* **23***,* 39-60.

Wiebe, E. C., and A. J. Weaver, 1999: On the sensitivity of global warming experiments to the parameterisation of sub-grid scale ocean mixing, *Clim. Dyn*., **15**, 875,893.

Wu, G.-X., X.-H. Zhang, H. Liu, Y.-Q. Yu, X.-Z. Jin, Y.-F. Guo, S.-F. Sun, and W.-P. Li, 1997: Global ocean-atmosphere-land system model of LASG (GOALS/LASG) and its performance in simulation study. *Quart. J. Appl. Meteor*., **8,** Supplement, 15-28 (in Chinese).

Zhang, J., R. W. Schmitt, and R. X. Huang, 1999: The relative influence of diapycnal mixing and hydrological forcing on the stability of the thermocline circulation, *J. Phys. Oceanogr.,* **29***,* 1096-1108.

Zhang, X.-H., G.-Y. Shi, H. Liu, and Y.-Q. Yu (eds.), 2000: IAP Global Atmosphere-Land System Model. Science Press, Beijing, China, 259 pp.

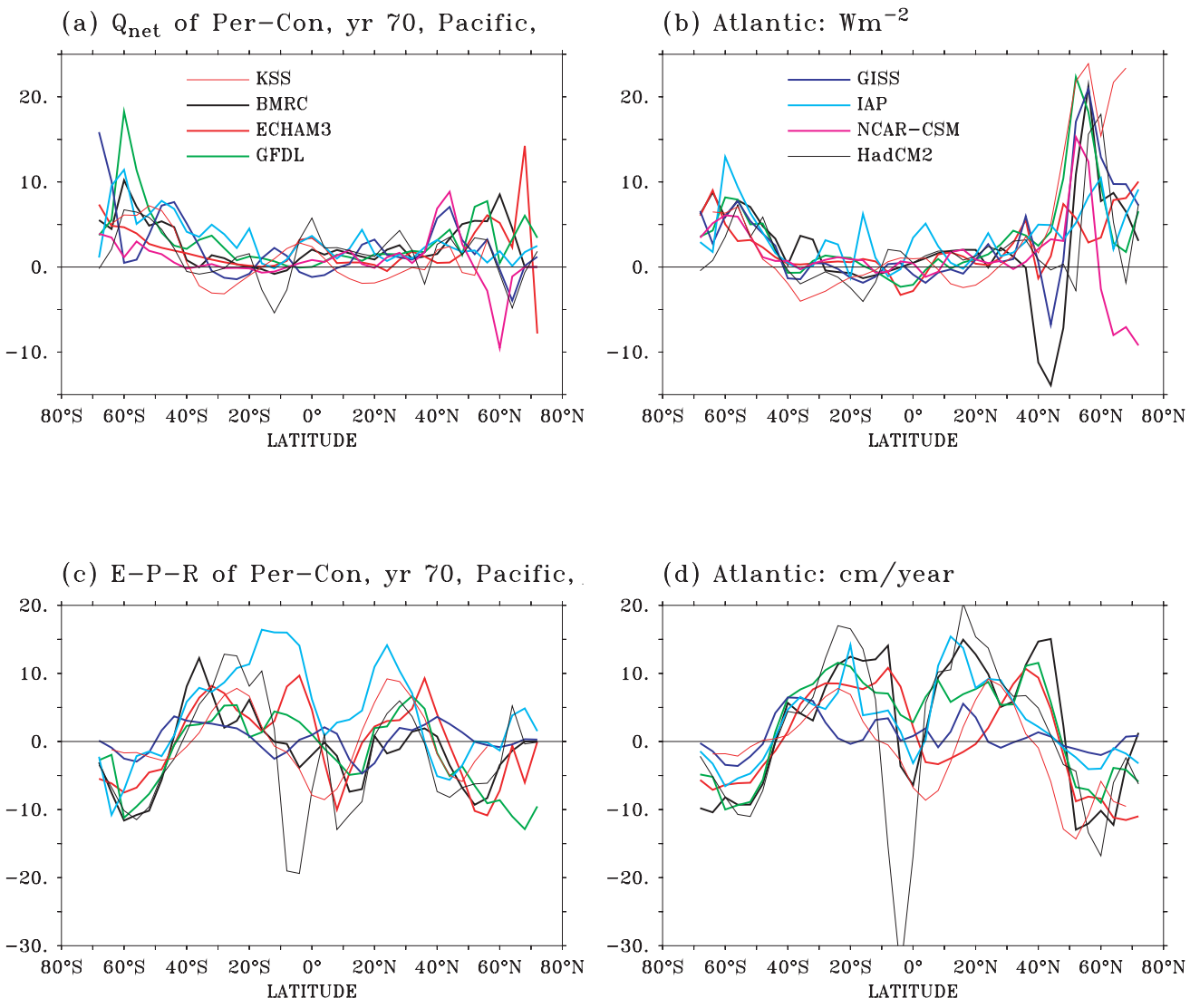


Fig. 1 Zonal averaged mean anomalies between 61 and 80 years except for KSS that is the annual average of year 70. (a) Downward net surface heat flux in the Pacific, and (b) in the Atlantic in unit of $Wm^{-2}$. (c) Freshwater flux (E-P-R) in the Pacific, and (d) in the Atlantic in unit of $cm/year$.

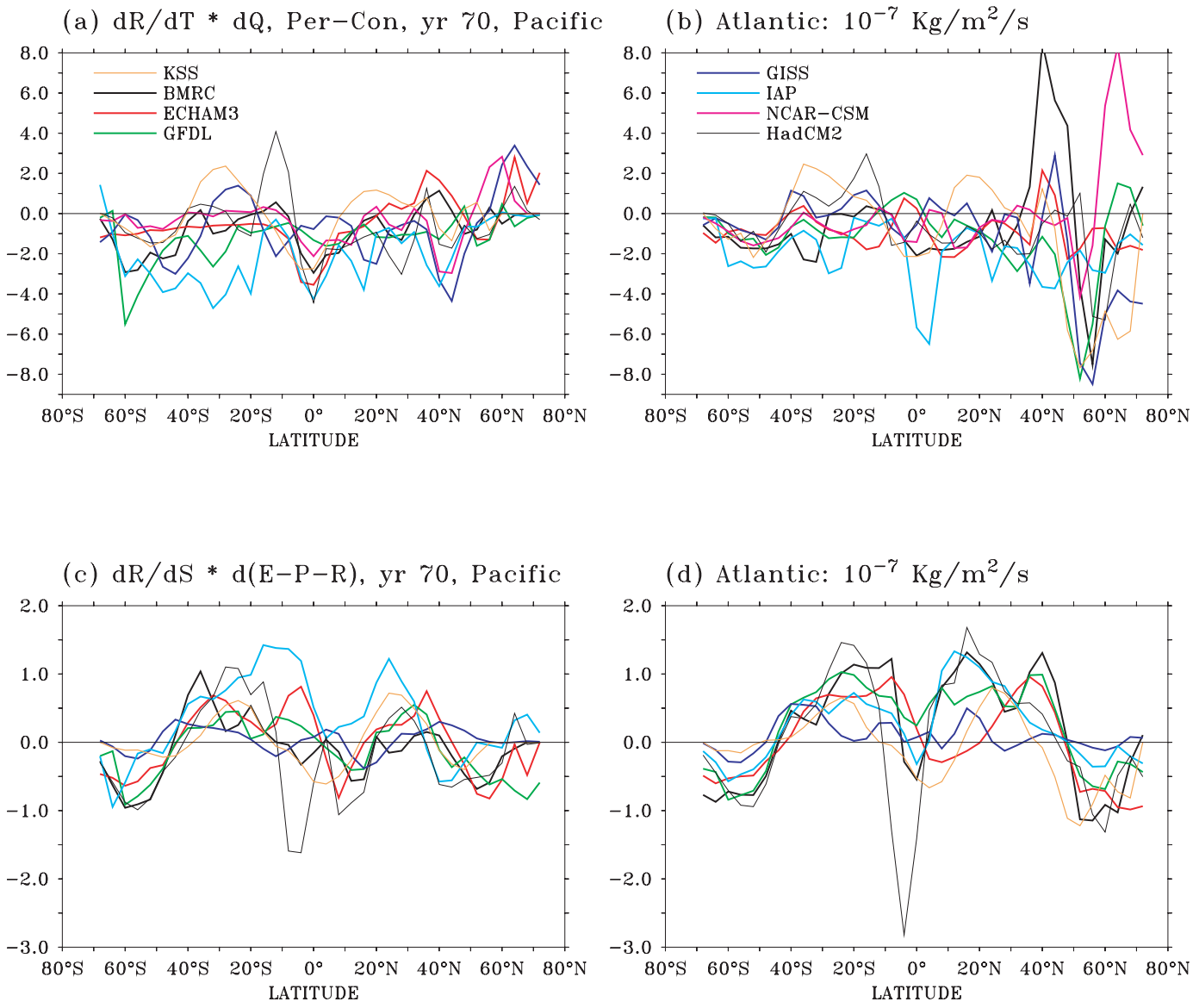


Fig. 2 Buoyancy flux (positive downwards) caused by (a) anomalous surface heat flux in the Pacific and (b) in the Atlantic, and by (c) anomalous freshwater flux in the Pacific and (d) in the Atlantic in unit of $10^{-7} Kgm^{-2}s^{-1}$. Values are zonally averaged mean between 61 and 80 years except for KSS which is the annual average for year 70.

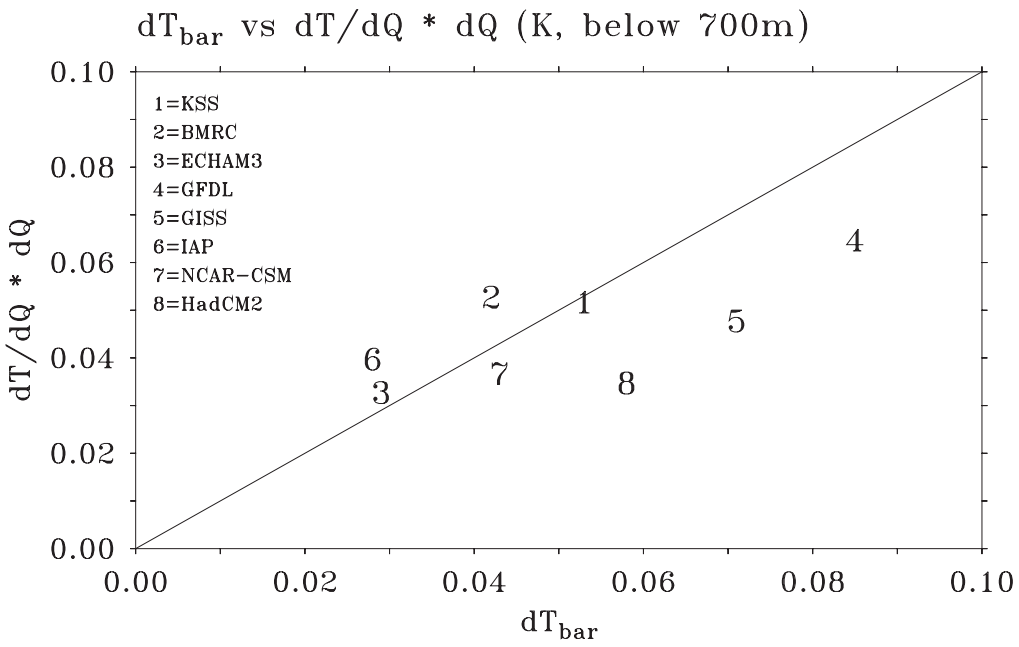


Fig. 3 Comparison of the DOHU below 700 m calculated from CMIP-2 simulations ($\Delta T$, x-axis) with that estimated by applying the adjoint sensitivity $(\partial \overline{T} / \partial Q_s)\Delta Q_s$ (y-axis).

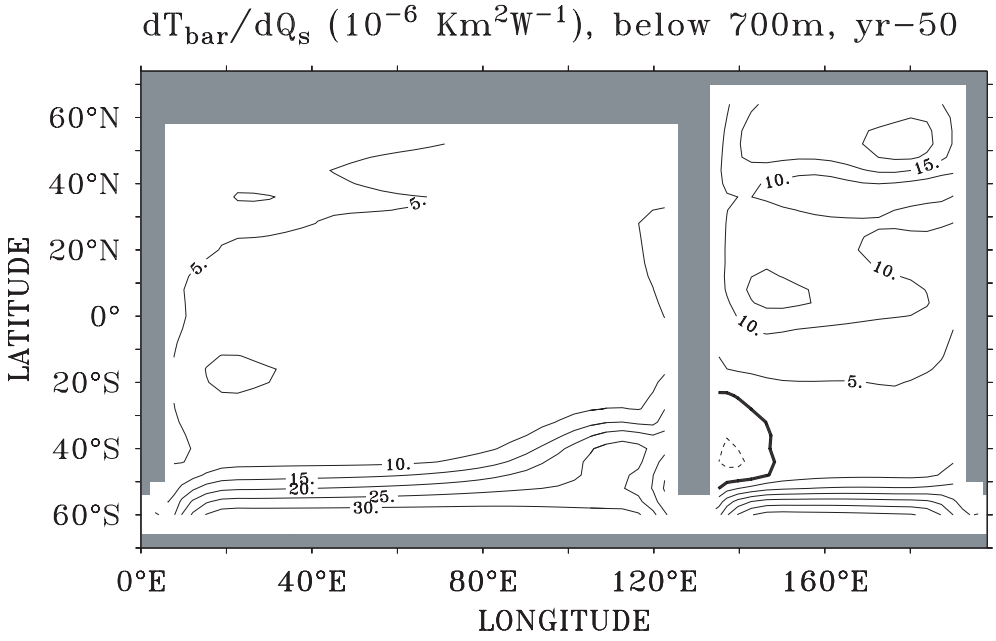


Fig. 4 Sensitivity of deep-ocean heat uptake below 700 m to the surface heat flux. Contour interval is $2\times10^{-6} Km^2W^{-1}$. The solid (dashed) contours represent positive (negative) values. The time scale for the sensitivity is 50 years.

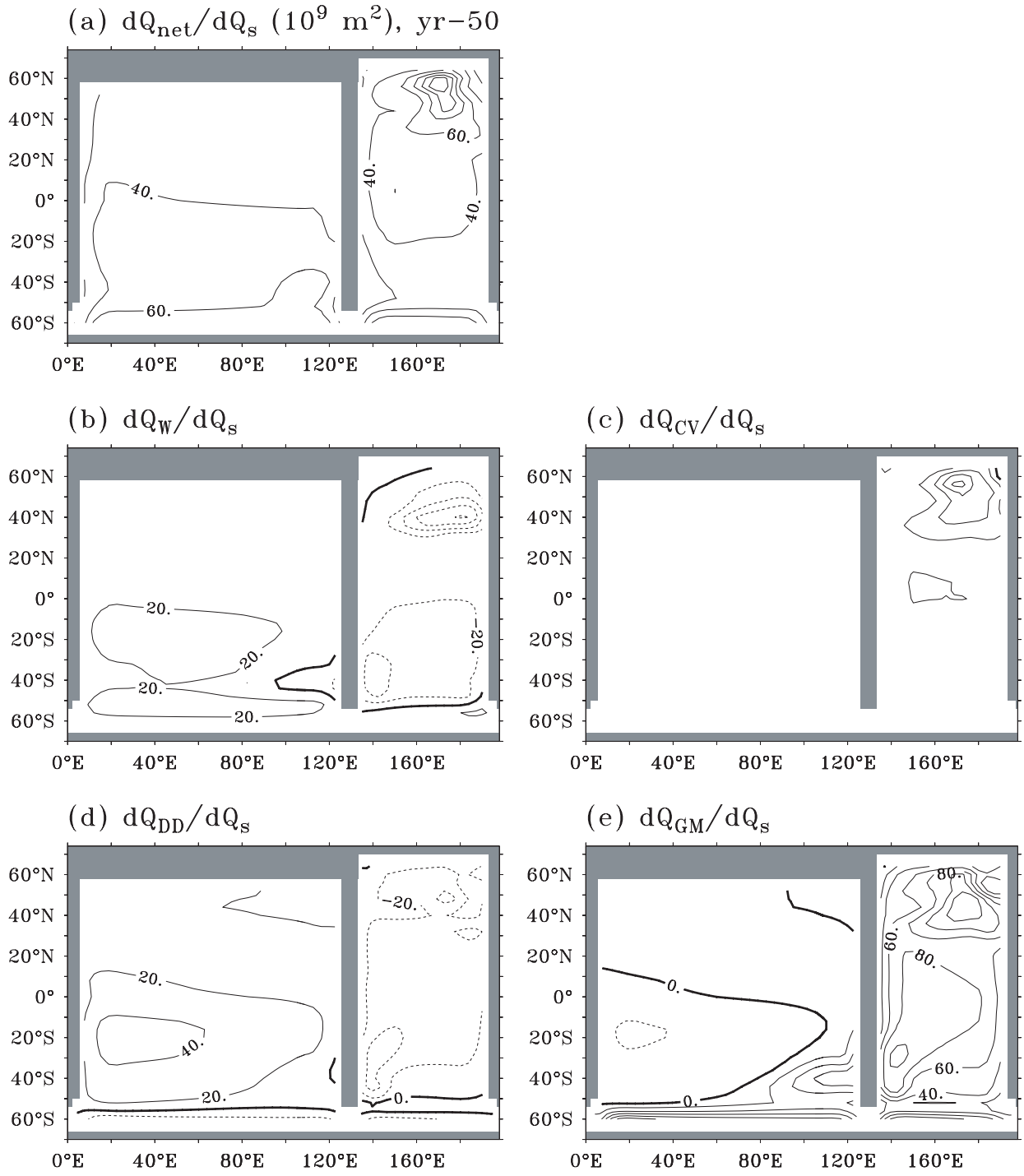


Fig. 5 Adjoint sensitivity of downward heat fluxes across 700 m to the surface heat anomaly at the time scale of 50 years. (a) Net heat flux. (b) Vertical advective heat flux. (c) Convective heat flux. (d) Diapycnal heat flux. (e) Eddy heat flux due to Gent-McWilliams mixing. The contour interval is $20\times10^{9}\,m^{-2}$.

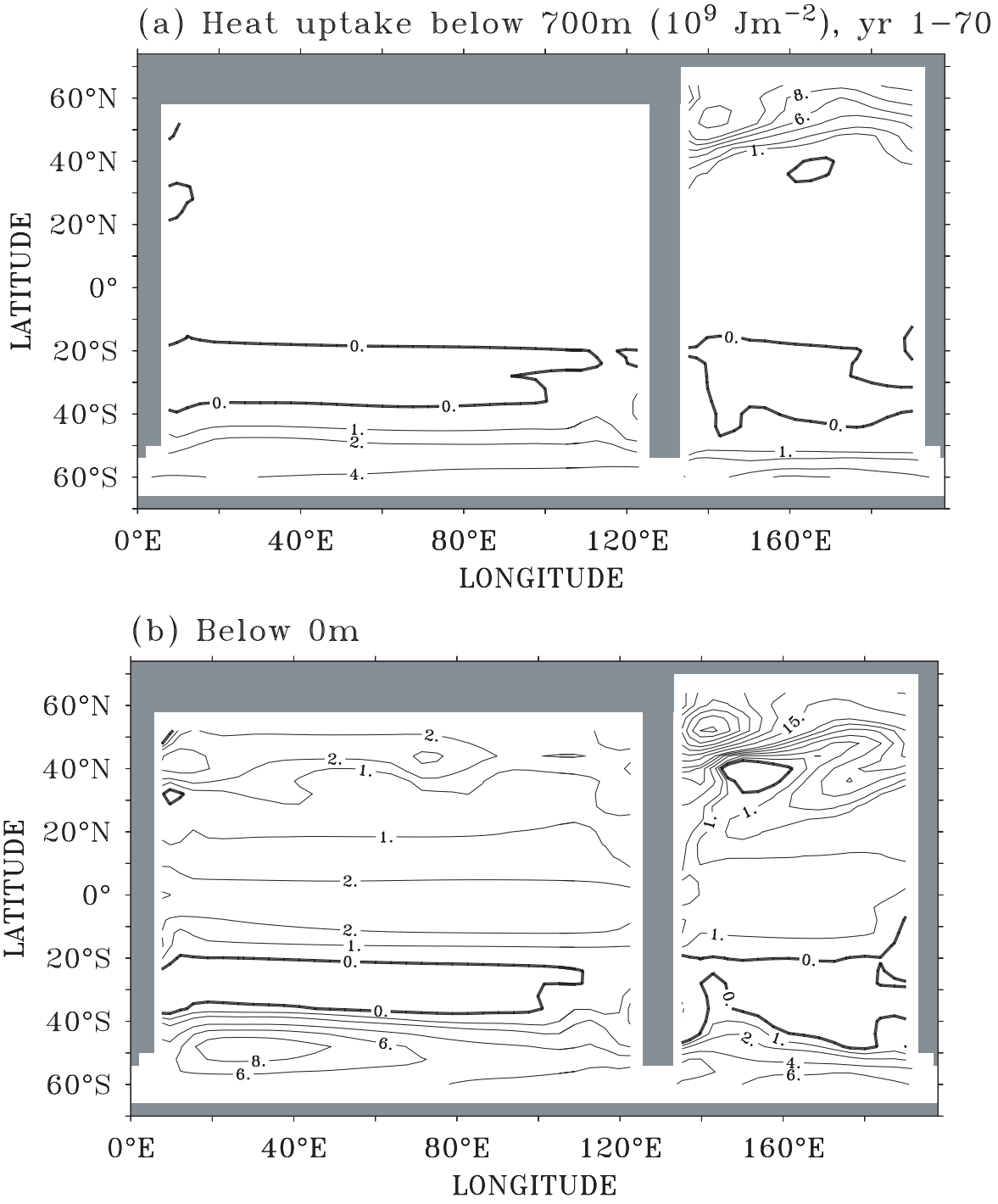


Fig. 6 Spatial distribution of ocean heat uptake within 70 years across (a) 700 m, and (b) 0 m. Contour intervals are 1 between 0 and 1, 2 between 2 and 10, and 5 between 15 and 50. Unit is $10^9 Jm^{-2}$.

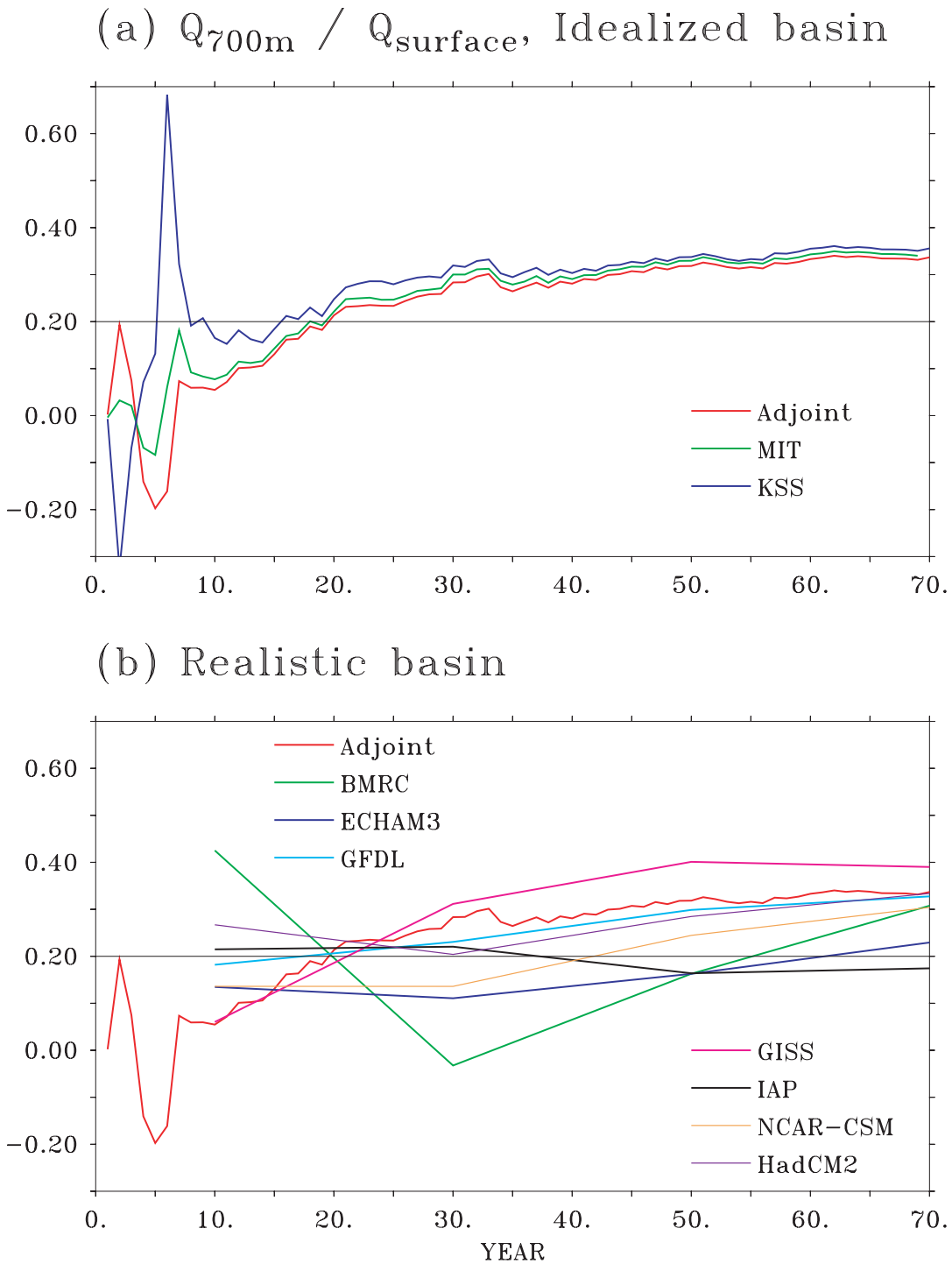


Fig. 7 Ratio between the deep-ocean heat uptake below 700 m and the total absorbed heat. (a) Models with an idealized basin. (b) Models with fully coupled GCMs and a realistic topography from CMIP-2.

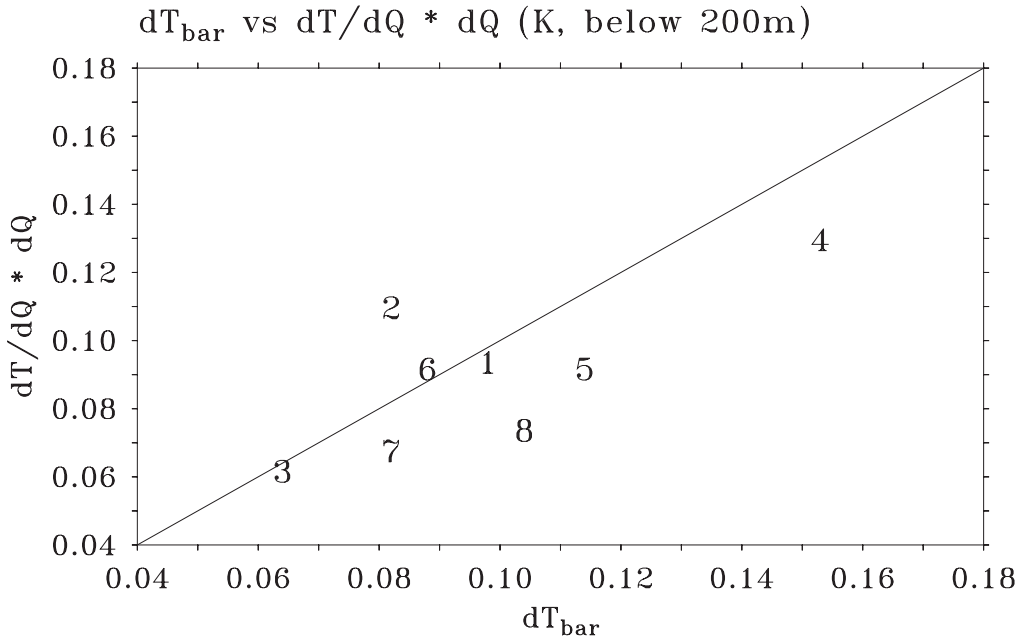


Fig. 8 Comparison of the DOHU below 200 m calculated by applying OGCM simulation $\Delta T$ (x-axis) with that estimated by applying adjoint sensitivity $(\partial \overline{T} / \partial Q_S)\Delta Q_S$ (y-axis).

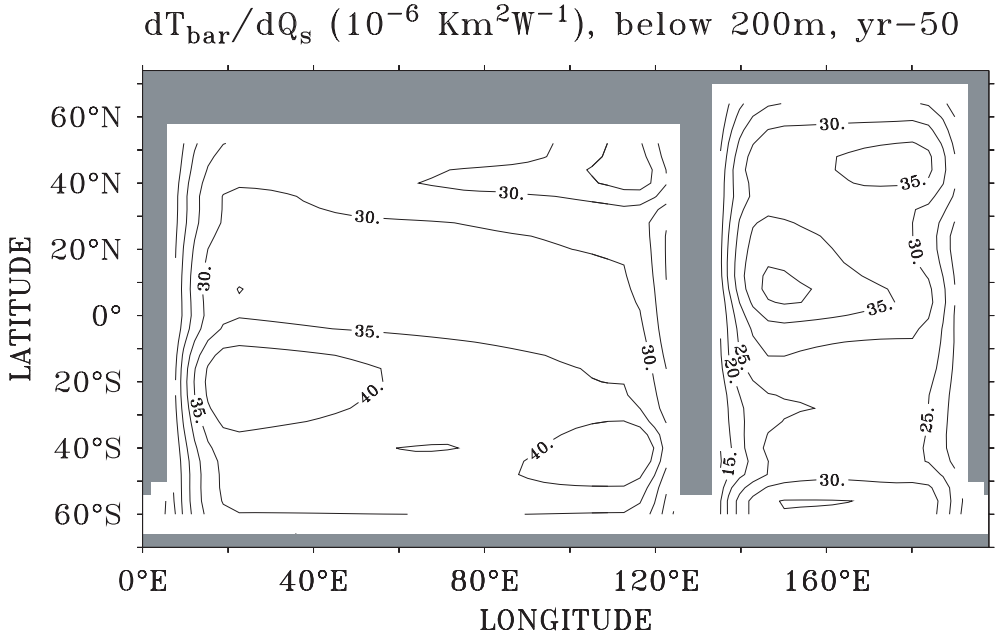


Fig. 9 Sensitivity of deep-ocean heat uptake below 200 m to the surface heat flux. Contour interval is $5\times10^{-6} Km^2W^{-1}$.

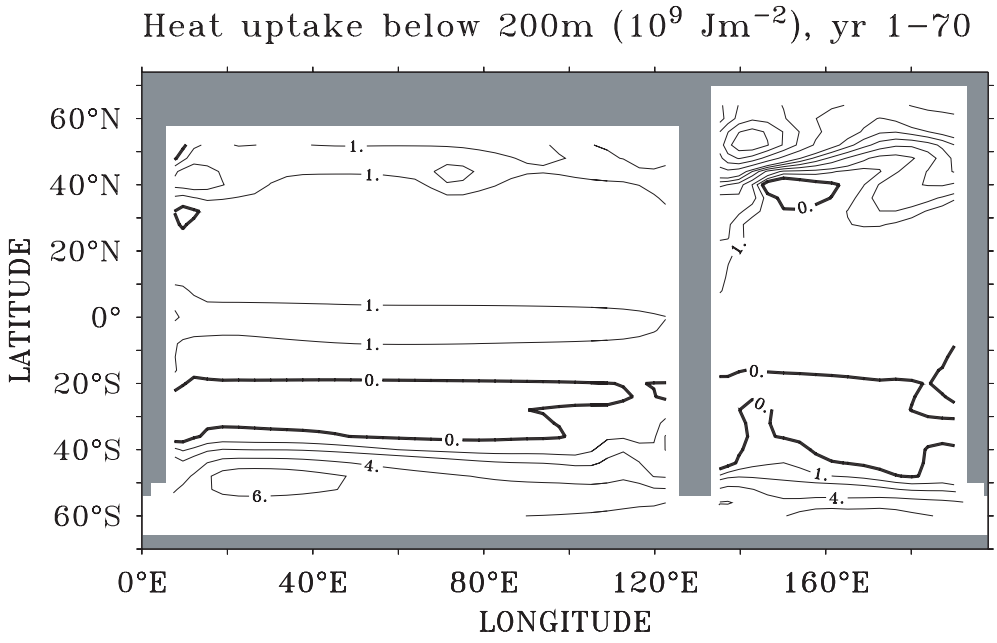


Fig. 10 Spatial distribution of ocean heat uptake across 200 m at time scale of 70 years. Contour intervals are 1 between 0 and 1, 2 between 2 and 10, and 5 between 15 and 50. Unit is $10^9 Jm^{-2}$.

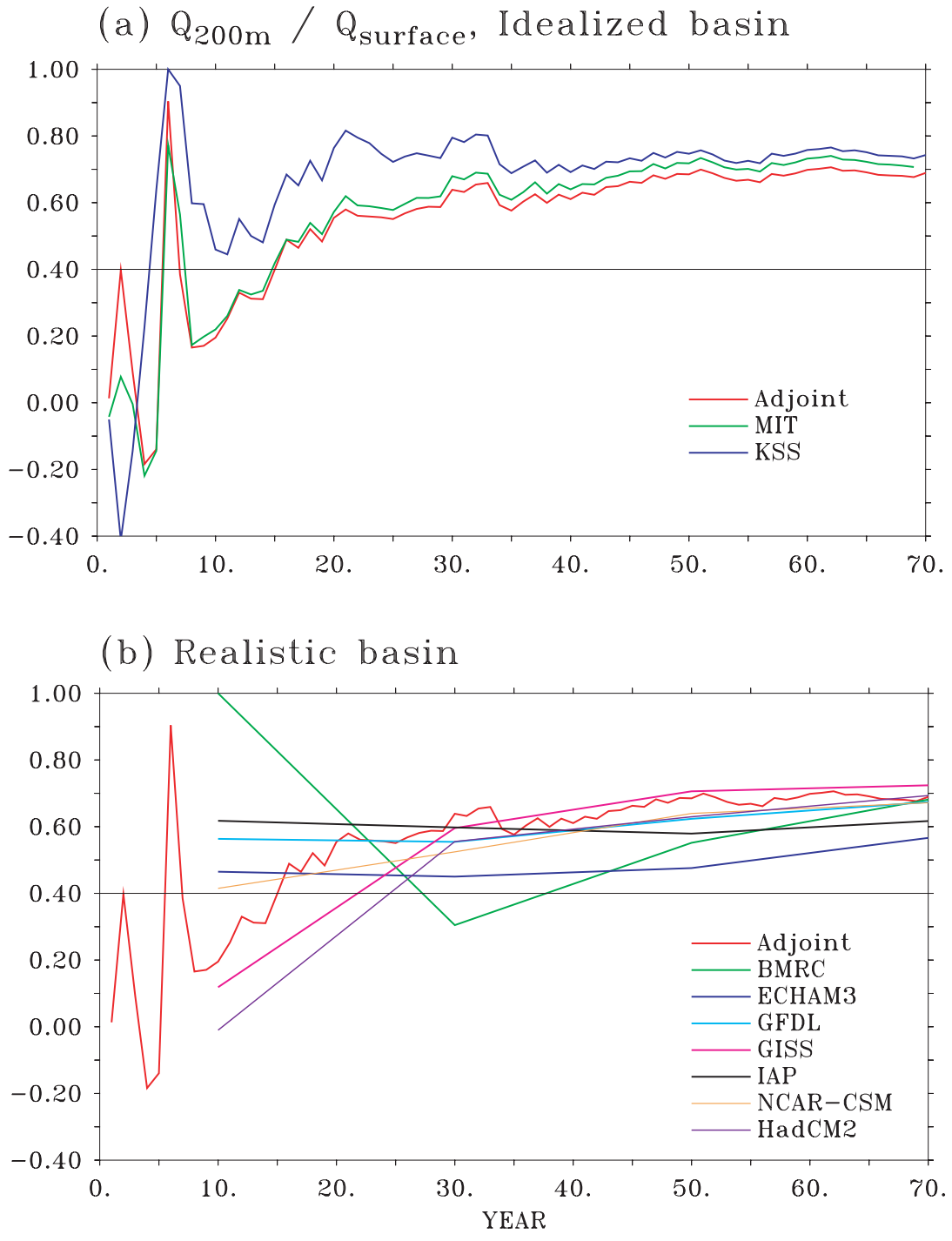


Fig. 11 Ratio between the deep-ocean heat uptake below 200 m and the total absorbed heat. (a) Models with an idealized basin. (b) Models with fully coupled GCMs and a realistic topography from CMIP-2.

Table 1. Estimated ocean heat uptake (°K) in different models at the time scale of 70 years. $\partial\overline{T}/\partial Q_S$ and $\partial\overline{T}/\partial F_S$ are the adjoint sensitivities of DOHU to surface heat and freshwater flux, respectively. $\Delta Q_S$, $\Delta F_S = \Delta(E-P-R)$, and $\Delta\overline{T}$ are the anomaly between perturbation and control runs. One-degree change of average temperature below 700 m (200 m) represents a DOHU of 3.7 (4.2) $\times 10^{24}$ J.

| | **Below 700 m** | | | **Below 200 m** | | |
|---|---|---|---|---|---|---|
| | $\frac{\partial\overline{T}}{\partial Q_S}\Delta Q_S$ | $\frac{\partial\overline{T}}{\partial F_S}\Delta F_S$ | $\Delta\overline{T}$ | $\frac{\partial\overline{T}}{\partial Q_S}\Delta Q_S$ | $\frac{\partial\overline{T}}{\partial F_S}\Delta F_S$ | $\Delta\overline{T}$ |
| KSS model | .052 | -.0010 | .053 | .094 | .00020 | .098 |
| BMRC | .053 | .00062 | .042 | .110 | .0024 | .082 |
| ECHAM3 | .033 | .0012 | .029 | .062 | .0022 | .064 |
| GFDL | .065 | .0019 | .085 | .130 | .0027 | .153 |
| GISS | .048 | .0011 | .071 | .092 | .00087 | .114 |
| IAP | .040 | -.000043 | .028 | .092 | .00099 | .088 |
| NCAR-CSM | .037 | N/A | .043 | .068 | N/A | .082 |
| HadCM2 | .035 | .0021 | .058 | .074 | .0029 | .104 |

## REPORT SERIES of the MIT *Joint Program on the Science and Policy of Global Change*

1. **Uncertainty in Climate Change Policy Analysis** *Jacoby & Prinn* December 1994
2. **Description and Validation of the MIT Version of the GISS 2D Model** *Sokolov & Stone* June 1995
3. **Responses of Primary Production and Carbon Storage to Changes in Climate and Atmospheric $CO_2$ Concentration** *Xiao et al.* October 1995
4. **Application of the Probabilistic Collocation Method for an Uncertainty Analysis** *Webster et al.* Jan 1996
5. **World Energy Consumption and $CO_2$ Emissions: 1950-2050** *Schmalensee et al.* April 1996
6. **The MIT Emission Prediction and Policy Analysis (EPPA) Model** *Yang et al.* May 1996
7. **Integrated Global System Model for Climate Policy Analysis** *Prinn et al.* June 1996 (*superseded by No. 36*)
8. **Relative Roles of Changes in $CO_2$ and Climate to Equilibrium Responses of Net Primary Production and Carbon Storage** *Xiao et al.* June 1996
9. **$CO_2$ Emissions Limits: *Economic Adjustments and the Distribution of Burdens*** *Jacoby et al.* July 1997
10. **Modeling the Emissions of $N_2O$ & $CH_4$ from the Terrestrial Biosphere to the Atmosphere** *Liu* Aug 1996
11. **Global Warming Projections: *Sensitivity to Deep Ocean Mixing*** *Sokolov & Stone* September 1996
12. **Net Primary Production of Ecosystems in China and its Equilibrium Responses to Climate Changes** *Xiao et al.* November 1996
13. **Greenhouse Policy Architectures and Institutions** *Schmalensee* November 1996
14. **What Does Stabilizing Greenhouse Gas Concentrations Mean?** *Jacoby et al.* November 1996
15. **Economic Assessment of $CO_2$ Capture and Disposal** *Eckaus et al.* December 1996
16. **What Drives Deforestation in the Brazilian Amazon?** *Pfaff* December 1996
17. **A Flexible Climate Model For Use In Integrated Assessments** *Sokolov & Stone* March 1997
18. **Transient Climate Change & Potential Croplands of the World in the 21st Century** *Xiao et al.* May 1997
19. **Joint Implementation: *Lessons from Title IV's Voluntary Compliance Programs*** *Atkeson* June 1997
20. **Parameterization of Urban Sub-grid Scale Processes in Global Atmospheric Chemistry Models** *Calbo et al.* July 1997
21. **Needed: A Realistic Strategy for Global Warming** *Jacoby, Prinn & Schmalensee* August 1997
22. **Same Science, Differing Policies; *The Saga of Global Climate Change*** *Skolnikoff* August 1997
23. **Uncertainty in the Oceanic Heat & Carbon Uptake & their Impact on Climate Projections** *Sokolov et al.* Sep 1997
24. **A Global Interactive Chemistry and Climate Model** *Wang, Prinn & Sokolov* September 1997
25. **Interactions Among Emissions, Atmospheric Chemistry and Climate Change** *Wang & Prinn* Sep 1997
26. **Necessary Conditions for Stabilization Agreements** *Yang & Jacoby* October 1997
27. **Annex I Differentiation Proposals: *Implications for Welfare, Equity and Policy*** *Reiner & Jacoby* Oct 1997
28. **Transient Climate Change & Net Ecosystem Production of the Terrestrial Biosphere** *Xiao et al.* Nov 1997
29. **Analysis of $CO_2$ Emissions from Fossil Fuel in Korea: 1961–1994** *Choi* November 1997
30. **Uncertainty in Future Carbon Emissions: *A Preliminary Exploration*** *Webster* November 1997
31. **Beyond Emissions Paths: *Rethinking the Climate Impacts of Emissions Protocols*** *Webster & Reiner* Nov 1997
32. **Kyoto's Unfinished Business** *Jacoby, Prinn & Schmalensee* June 1998
33. **Economic Development and the Structure of the Demand for Commercial Energy** *Judson et al.* April 1998
34. **Combined Effects of Anthropogenic Emissions and Resultant Climatic Changes on Atmospheric OH** *Wang & Prinn* April 1998
35. **Impact of Emissions, Chemistry, and Climate on Atmospheric Carbon Monoxide** *Wang & Prinn* Apr 1998
36. **Integrated Global System Model for Climate Policy Assessment: *Feedbacks and Sensitivity Studies*** *Prinn et al.* June 1998
37. **Quantifying the Uncertainty in Climate Predictions** *Webster & Sokolov* July 1998
38. **Sequential Climate Decisions Under Uncertainty: *An Integrated Framework*** *Valverde et al.* Sep 1998
39. **Uncertainty in Atm. $CO_2$ (Ocean Carbon Cycle Model Analysis)** *Holian* Oct 1998 (*superseded by No. 80*)
40. **Analysis of Post-Kyoto $CO_2$ Emissions Trading Using Marginal Abatement Curves** *Ellerman & Decaux* Oct 1998
41. **The Effects on Developing Countries of the Kyoto Protocol & $CO_2$ Emissions Trading** *Ellerman et al.* Nov 1998
42. **Obstacles to Global $CO_2$ Trading: *A Familiar Problem*** *Ellerman* November 1998
43. **The Uses and Misuses of Technology Development as a Component of Climate Policy** *Jacoby* Nov 1998
44. **Primary Aluminum Production: *Climate Policy, Emissions and Costs*** *Harnisch et al.* December 1998
45. **Multi-Gas Assessment of the Kyoto Protocol** *Reilly et al.* January 1999
46. **From Science to Policy: *The Science-Related Politics of Climate Change Policy in the U.S.*** *Skolnikoff* Jan 1999

***Contact the Joint Program Office to request a copy. The Report Series is distributed at no charge.***